Turbulence and Transport in Simple Magnetized Toroidal Plasmas

I. Furno, A. Diallo, A. Fasoli, D. Iraji, B. Labit, S. H. Müller, G. Plyushchev, M. Podestà, F.M. Poli, P. Ricci, C. Theiler

Ecole Polytechnique Fédérale de Lausanne (EPFL), Centre de Recherches en Physique des Plasmas, Association EURATOM-Confédération Suisse, CH-1015 Lausanne, Switzerland

email contact of main author: ivo.furno@epfl.ch

Abstract: Progress in understanding turbulence and related cross-field transport of fusion relevance is achieved in the simple magnetized plasmas of the TORPEX toroidal device, which provides an ideal test bed for code benchmarking and theory validation. In TORPEX (R = 1 m, a = 0.2 m), a small vertical magnetic field $B_z < 4$ mT is superposed on a toroidal magnetic field B_t < 100 mT, resulting in open helical magnetic field lines. Similarly to the Scrape-Off Layer of fusion devices, ∇B and magnetic field curvature are at play. Here, Hydrogen plasmas are produced by microwaves (2.45 GHz, P<10 kW) with electron temperatures ~5 eV and densities ~1×10^{16} m^{-3}. Drift and interchange instabilities are observed and characterized in terms of dispersion relation, driving mechanisms and non-linear development into turbulence and blobs. Density fluctuations associated with drift-interchange waves exhibit universal statistical properties. Their probability density functions (PDFs) are best fitted by a Beta distribution, with a unique quadratic polynomial relation linking their skewness and flatness. At large vertical fields, PDFs with positive skewness are associated with blobs, which form from radially elongated structures that are sheared off by the ***E***x***B*** flow. These structures are in turn generated by interchange waves that increase in amplitude and extend radially following an increase of the radial pressure gradient. The transport of heat and particles associated with the interchange wave and the blobs is investigated, revealing that fundamentally different mechanisms are involved. Initial fluid simulations of the interchange-dominated regime show intermittent transport in the presence of plasma blobs.

1. Introduction

Fusion research is advanced by activities directly related to ITER developments, experiments investigating integrated scenarios, and by combined experimental and theoretical studies of fundamental phenomena, in particular in the area of plasma confinement. Cross-field transport of particles and heat in magnetically confined plasmas for fusion is anomalous, i.e. much larger than the transport induced by collisional processes and attributed to plasma turbulence. The limited diagnostic access in fusion devices has stimulated, in recent years, investigations of plasma turbulence in basic plasma physics devices, in which full diagnostic access with adequate spatial and temporal resolution can be obtained, thus providing a test bed for code and theory verification.

Here, we report on recent progress in understanding fundamental aspects of fluctuations, turbulence and related transport in simple magnetized plasmas of the TORPEX toroidal device [1] with a particular focus on the interchange-dominated regime, which has aspects that are in common with the Scrape-Off Layer (SOL) of fusion devices, such as intermittent transport associated with plasma blobs [2,3]. The remainder of the paper is organized as follows. In Sec. II, the TORPEX device and diagnostics are described. In Sec. III, the nature of electrostatic fluctuations and their universal aspects are elucidated using both spectral and statistical methods. In Sec. IV and V, we describe the main feature of the interchange dominated regime and we detail the blob generation mechanism. The transport associated with coherent interchange waves and blobs is discussed in Sec. VI and first numerical simulations are presented in Sec. VII. Conclusions are offered in Sec. VIII, along with an outlook.

2. The TORPEX device and diagnostics

The TORPEX device [1] has been built with the aim of contributing to bridging the gap between plasma turbulence experiments and simulations. TORPEX (R = 1 m, a = 0.2 m) is a toroidal device in which a small vertical magnetic field $B_z \leq 4$ mT is superposed on a toroidal magnetic field $B_t \leq 100$ mT to form helical magnetic field lines whose both ends terminate on the vessel. Similarly to the SOL of toroidal fusion devices, this magnetic configuration, usually referred to as simple magnetized torus (SMT), features open field lines, ∇B, and magnetic field curvature. Plasmas of different gases are produced by microwave power (P_{RF}<10 kW) injected from the low-field side at 2.45 GHz, in the electron-cyclotron frequency range. Here, we focus on Hydrogen plasmas, which are characterized by electron temperatures $T_e \sim$ 5-15 eV and densities $n_e \sim 3\times10^{16}$ m^{-3}. Extensive sets of Langmuir probes are used to characterize electrostatic fluctuations in terms of linear dispersion relation, statistical properties, and non-linear wave-wave interactions. In particular, full spatio-temporal imaging of electrostatic fluctuations is performed using both an array of 86 Langmuir probes, dubbed HEXTIP, which provides a complete coverage of the poloidal cross section, and via conditional sampling of data obtained from movable probes.

3. Nature of instabilities and universality of fluctuations

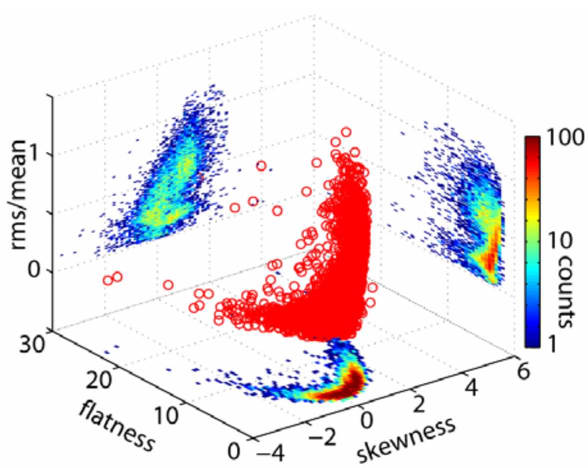

FIG. 1. 3D scattered plot of skewness vs flatness vs r.m.s /mean for around 10000 time series of electron density measured in various experimental conditions (red dots). On each plane, it is shown the histogram for the three combinations of parameters.

In recent years, a significant effort has been dedicated to investigating the nature (drift versus interchange driven instabilities) and universal features of fluctuations in the SOL/edge of fusion devices. The SMT configuration provides a drive for both drift and interchange instabilities [4]. These instabilities, fully characterized in terms of dispersion relation, driving mechanisms, and nonlinear development into turbulence, are observed to co-exist in TORPEX plasmas in the unfavourable curvature region [5]. A regime transition between drift and interchange waves is observed as the vertical magnetic field strength is varied [5]. Drift instabilities dominate for low vertical field values (B_z < 0.6 mT for Hydrogen plasmas), while interchange instabilities dominate for high vertical field values, B_z>1.4 mT. The observed transition is theoretically reproduced by a two-fluid model, based on the drift-reduced Braginskii equations [5].

Statistical properties are investigated over a broad range of experimental conditions using electron density fluctuation measurements, which are taken across the entire plasma cross section. The results are summarized in Fig. 1, which shows a 3D scattered plot of skewness, S, (third moment of the probability density function (PDF) of the fluctuations) vs flatness, F, (fourth moment of the PDF), vs the root-mean-square of the fluctuations normalized to their time-averaged value for around 10000 time series of electron density signals (red dots). While no clear dependence of F upon the normalized fluctuation level is observed, we find a correlation between the latter and the skewness: large values of r.m.s. / $\langle n \rangle$ corresponds to large S values. Moreover, a unique quadratic relation links S and F: $F=1.502S^2 + 2.78$, which constitues a first evidence of universality. Fluctuations in the drift-interchange frequency domain are necessary and sufficient to retrieve the observed quadratic relationship [6]. The second evidence of universality is that density fluctuation PDFs from all locations can be described by the same analytical distribution, which is a special case of the general Beta distribution. For positive skewness, this PDF reduces to the Gamma distribution, consistent with previous observations in the tokamak SOL [6].

4. Interchange-dominated regime: blobs and interchange waves

In the following, we focus on the interchange-dominated regime, achieved through relatively high values of B_z and showing similarities with the SOL of fusion devices [2, 3, 7]. In particular, we observe bursty transport, which is associated with the propagation of isolated structures, in which density and temperature are larger than in the surrounding plasma. These structures, dubbed blobs, extend along the field lines and propagate away from the plasma core resulting in outward heat and particle transport.

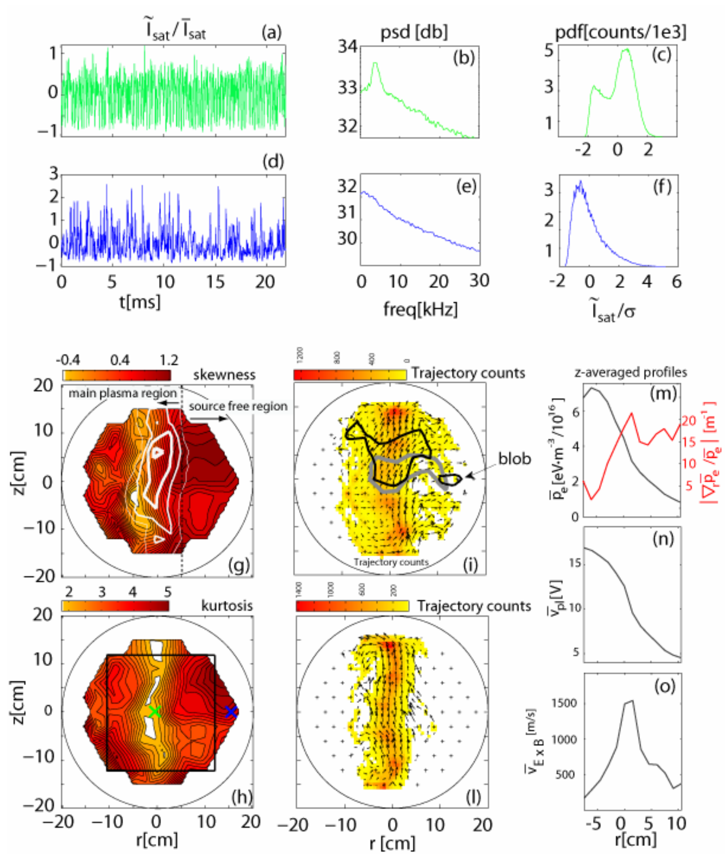

FIG. 2. (a, d) I_{sat} signals at the two locations indicated in (h) show coherent fluctuations in the main plasma region (green cross) and intermittent bursts at the edge (blue cross). Also shown are the respective PDFs in (c, f) and the power spectral densities in (b, e). Poloidal profiles of (g) skewness and (h) flatness of I_{sat} signals. In (g) the profile (white) of spectral power in the frequency range 3.9+/-1 kHz localizes the interchange wave. Contours correspond to 90%, 60%, 30%, and 10% of the maximum spectral power. Mean velocity field of positive (i) and negative (l) structures and histogram (color) of trajectory counts. (m-o) z-averaged profiles of various quantities.

In Fig. 2 we illustrate statistical and spectral properties of fluctuations, together with time-averaged profiles in the interchange-dominated regime. A low microwave power (400 W) is used in a toroidal magnetic field of 76 mT on axis and a vertical magnetic field B_z = 2.3 mT, which results in a vertically elongated plasma configuration with the plasma source localized on the high field side (HFS), with negligible plasma production for r>5 cm. Figure 2 (a-l) shows statistical and spectral properties of ion saturation, I_{sat}, signals. Figure 2(m-o) shows z-

averaged profiles of the time-averaged electron pressure $p_e = n_e T_e$, inverse pressure radial scale-length $|L_{pe}|^{-1} = |\nabla_r p_e / p_e|$, plasma potential V_{pl}, and the ***E***x***B*** velocity, v_{ExB}, obtained from Langmuir probe measurements.

The 2D profiles of skewness *S*, Fig. 2(g), and flatness *F*, Fig. 2(h), of I_{sat} signals clearly identify two distinct poloidal regions with different plasma dynamics: 1) a main plasma region for $-5 \le r \le 5$ cm which is dominated by a coherent interchange wave; 2) a region on the low-field side for $r > 5$ cm with negligible plasma production, dubbed source-free region, which, as discussed below, is characterized by the propagation of plasma blobs. Fig. 2(a) shows I_{sat} fluctuations in the main plasma region that are dominated by coherent oscillations at a frequency of ~3.9 kHz, as confirmed by the power spectral density in Fig. 2 (b). The PDF in Fig. 2 (c) is double-humped with $S \sim 0$ and $F \sim 2$, as expected for coherent fluctuations. The 2D profile of the spectral power in the range f=3.9 +/- 0.5 kHz is shown in Fig. 2 (g) and peaks around the position of maximum $|L_{pe}|^{-1}$, where it represents approximately 50% of the total spectral power of the fluctuating signal.

The nature of fluctuations in the source-free region can be inferred from the data shown in Fig. 2(i-l), representing the mean velocity field of positive and negative plasma structures identified using a pattern-recognition method combined with statistical analysis [8]. A positive structure example is shown in gray in Fig. 2(i). In the main plasma region, the trajectory patterns for positive and negative structures are very similar, consistently with the presence of the interchange wave. On the other hand, in the source-free region only positive structures — the blobs — have a significant probability of occurrence. In Fig. 2(i), the gray structure shears off and generates two structures (black line). The black structure at the low field side is a newly born blob. As shown by the trajectory pattern of the positive structures in Fig. 2(i), blobs propagate outwards in the source-free region as individual coherent structures over distances of the order of the minor radius.

Blob properties, such as speed and size, have been extensively studied analytically and numerically in the SOL of fusion devices (see the review article [9]). Sheath-connected blob models predicts that only blobs with a radius $a_b \approx \rho_s \left[L^2/(\rho_s R)\right]^{1/5}$ can travel as coherent structures over large distances [9]. For the plasma investigated here ($T_e \sim 4$ eV in the source-free region, $L \sim 13$ m), we find $a_b \sim 2.5$ cm, which is in agreement with the blob size found in the experiments. Scaling of the cross-field blob speed with size, connection length and base pressure for different gases are presently under investigation and will provide a test bed for semi-analytical blob models and numerical simulations.

5. Interchange-dominated regime: blob generation mechanism

The mechanism for blob generation is investigated using time resolved 2D profiles of n_e, T_e, V_{pl} and velocity fields, which are obtained by performing a conditional sampling over many blob events of the *I*-*V* characteristic of a Langmuir probe in a time window centered around the blob detection [3]. We point out that indirect evidence has been recently obtained in tokamaks that blobs are generated in the vicinity of the last closed flux surface, presumably as a result of interchange instability [10]. Therefore the present results may shed light on the blob ejection mechanism in tokamaks. The results of the conditional sampling technique shown in Fig. 3 capture the dynamics of blob formation and ejection from the interchange wave. Figure 3(a-d) shows 2D profiles of δn_e at four different times during the ejection of the blob together with the total ***E***x***B*** velocity field. Figure 3(e) shows the time evolution of δn_e in the mode region (red) and in the source-free region (black).

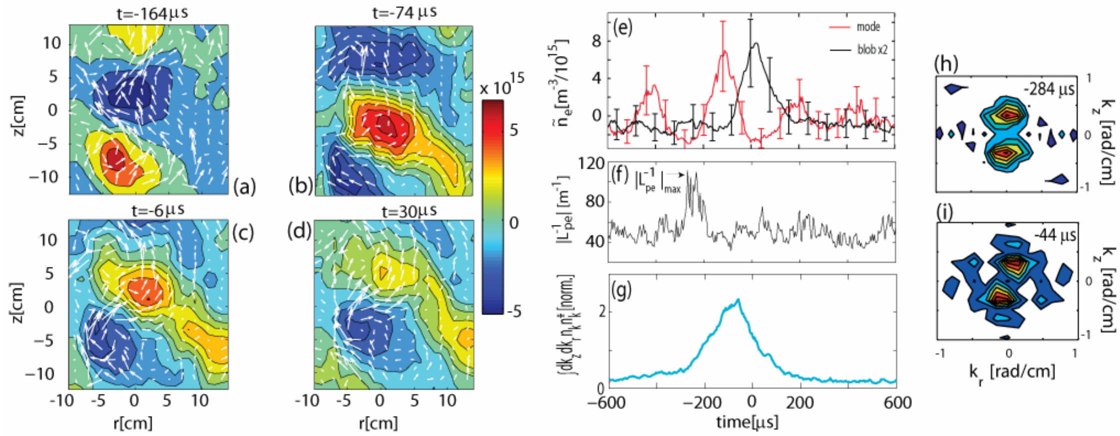

FIG. 3. Plasma dynamics from the conditional sampling technique. Shown are: (a)–(d) 2D profiles of δn_e at different times during blob ejection. The arrows show the instantaneous ***E****x****B*** *velocity; (e) time history of δn_e in the mode region (red) and in the source-free region (black). The latter is multiplied by two for clarity. Time evolution of (f) inverse pressure gradient length $|L_{pe}|^{-1}$ at the point of maximum observed intensity and of (g) mode amplitude. (h ,i) Decomposition in k-space of the density fluctuations at two different time frames.*

The coherent structures in Figs. 3(a) and 3(b) are identified with the interchange wave, based on their spatiotemporal properties. The formation of the elongated structure in Fig. 3(c) follows from an increase of the amplitude of the interchange wave, Fig. 3(g), which also extends radially in response to a decrease of the radial pressure local scale length, Fig. 3(f). The elongated density structure is convected upward in a sheared velocity field that moves HFS and LFS parts of the density structure with different vertical velocities. A relative displacement between them is obtained, Fig. 3(d), which results in a tilting and stretching of the structure. This is also consistent with a spatial Fourier harmonics (*k*-space) analysis, which shows that the radial wavenumber of the fluctuating density linearly *drifts* towards larger values during this phase [11]. Fig. 3(h, i) presents the 2D distribution of the decomposition in k-space of the density fluctuations at two different time frames during blob ejection. Eventually, the original density structure breaks into two parts, and the new structure on the low field side forms a plasma blob.

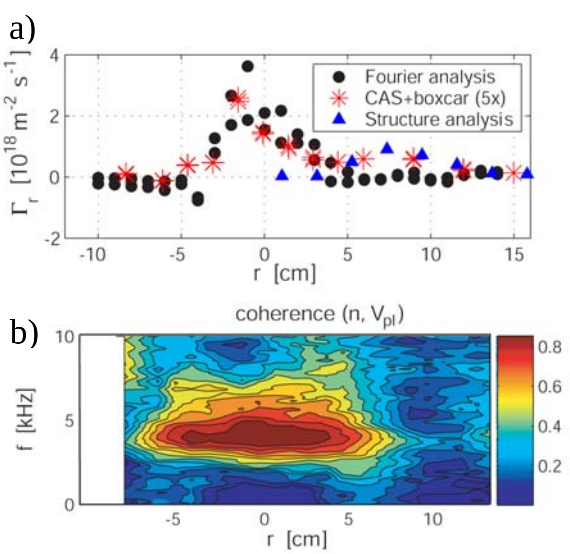

FIG. 4. Radial particle flux at mid plane measured by different techniques (top). Coherence between density and plasma potential fluctuations from Fourier analysis (bottom).

6. Transport of heat and particles associated with the interchange wave and the blobs

In the main plasma, which includes particle and heat sources, transport is dominated by the fluctuation-induced particle and heat flux associated with the interchange wave. In the source-free region, the cross-field transport is mainly due to the intermittent ejection of blobs propagating toward the outer wall. The transport caused directly by instabilities constitutes a fundamentally different mechanism from that mediated by blob formation [12].

Different techniques are used to investigate the physics underlying the cross-field transport associated with the interchange mode and with the blobs. A fluctuation-induced flux is found in the main plasma, Fig. 4(a). Here a finite coherence between fluctuations of n_e and plasma potential V_{pl} associated with the interchange mode is measured (Fig. 4-b). At the far LFS the time-averaged coherence approaches zero. Nevertheless, propagating blobs are also found to cause a radially outward flux, Fig. 4(a). Considering the typical blob lifetime, velocity and occurrence rate, the associated time-averaged transport is ≤4% of the total losses. Note that a similar fraction in fusion-oriented devices may induce large heat losses, and possible damages of in-vessel components. Instabilities and blobs constitute different mechanisms for anomalous cross-field transport, although the latter is basically related to the coupled dynamics of n_e and V_{pl} for both phenomena.

7. Theory modelling and numerical simulations

These findings have stimulated a theoretical approach to TORPEX turbulence based on fluid simulations [13]. Owing to the low plasma temperature in the TORPEX device, the drift-reduced Braginskii equations (see, e.g. [14]) can be used to model the plasma dynamics. The easiest turbulence regime to model is the one dominated by the interchange dynamics, which, since $k_{//}=0$, can be described by simple two-dimensional fluid equations. We assume $B_z<<B_T$, so that $B\sim B_0R/r$, and note that magnetic curvature is constant along a field line and equal to $1/R$. Here, we denote the radial direction with x, the parallel direction with z, and the direction perpendicular to x and z with y. The Braginskii equations are integrated in the parallel direction in order to evolve the line-integrated density, $n(x,y)=\int n(x,y,z)dz/L_c$, potential $\phi(x,y)=\int \phi(x,y,z)dz/L_c$, and temperature, $T_e(x,y)=\int T_e(x,y,z)dz/L_c$, $L_c=2\pi NR$ being the magnetic field line length. We use the Bohm's boundary conditions to take into account the ion and electron parallel flow at the sheath edge. By assuming that the density at the sheath entrance is equal to $n(x,y)/2$, it is possible to approximate the ion and electron flows as $\Gamma_{//,i}=nc_s/2$ and $\Gamma_{//,e}=nc_s\exp(-e\phi/T_e+\Lambda)/2$, with $\Lambda=\log\sqrt{m_i/(2\pi m_e)}$ [15]. Furthermore, we make use of the Boussinesq approximation [16] for the polarization drift, i.e.

$$\nabla\cdot\left(\frac{nm_i}{eB}\frac{d}{dt}\frac{\nabla\phi}{B}\right)=\frac{nm_i}{eB^2}\frac{d}{dt}\nabla^2\phi .$$

The evolution equations for T_e, n, and ϕ thus become

$$\frac{dT_e}{dt}=[\frac{c\phi}{B_0},T_e]+\frac{4c}{3eRB_0}\left(\frac{7}{2}T_e\frac{\partial T_e}{\partial y}+\frac{T_e^2}{n}\frac{\partial n}{\partial y}-T_e\frac{\partial\phi}{\partial y}\right)+\kappa_e\nabla^2T_e$$
$$-\frac{2}{3}\frac{\sigma T_e c_s}{R}[1.71\exp(\Lambda-e\phi/T_e)-0.71]+S_T$$
$$\frac{dn}{dt}=[\frac{c\phi}{B_0},n]+D_n\nabla^2n+\frac{2c}{eRB_0}\left(n\frac{\partial T_e}{\partial y}+T_e\frac{\partial N}{\partial y}-n\frac{\partial\phi}{\partial y}\right)-\frac{\sigma nc_s}{R}\exp(\Lambda-e\phi/T_e)+S_n$$
$$\frac{d\nabla^2\phi}{dt}=[\frac{c\phi}{B_0},\nabla^2\phi]+\nu\nabla^4\phi+\frac{2B_0}{cm_iR}\left(\frac{T_e}{n}\frac{\partial n}{\partial y}-\frac{\partial T_e}{\partial y}\right)+\frac{\sigma c_s m_i\Omega_i^2}{eR}[1-\exp(\Lambda-e\phi/T_e)] .$$

Here S_n and S_T represent particle and heat sources, $\sigma = R / L_c = \Delta / (2\pi L_v)$, and $[a,b] = \partial_x a \partial_y b - \partial_y a \partial_x b$. We note that a similar system of equations has been used in [17]. The system of equations is solved numerically, via a finite difference scheme, using source profiles that mimic the Electron Cyclotron and Upper Hybrid resonance layers in TORPEX. The plasma and heat sources increase the plasma pressure, thus enhancing the pressure gradient and triggering the interchange instability. The interchange instability leads to density and heat transport from the source region to the low field side of the machine. Cross-field transport appears intermittent, with the presence of plasma blobs that propagate in the radial direction.

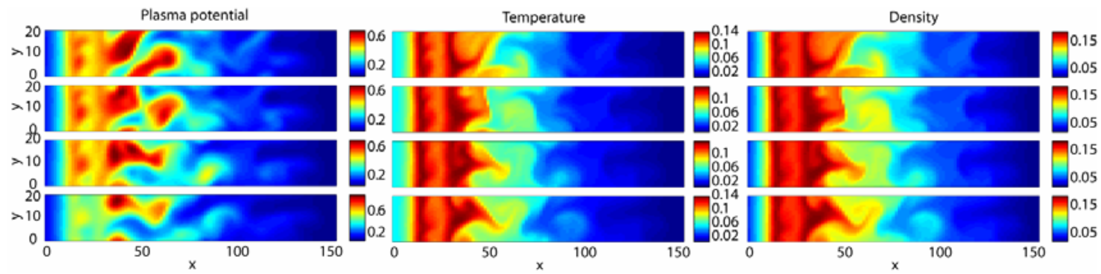

FIG. 5. A typical intermittent transport event from simulations. Different rows correspond to different times.

A typical intermittent transport event, as modelled in the fluid code, is shown in Fig. 5 through snapshots of the potential, temperature, and density. Corresponding to these plasma intermittent transport events, a skewed probability distribution function for the density is observed on the low field side of the machine. We note that, while the plasma is transported in the radial direction by the interchange dynamics, it is removed from the system by parallel losses. The simulations show that, after a transient, an equilibrium profile is established as a result of a balance between parallel losses, perpendicular transport, and sources. In particular, quasi-neutrality leads to a link between the equilibrium potential and temperature profiles, i.e. $\phi \approx \Lambda T_e$ that is also observed experimentally.

8. Conclusions and outlook

We have detailed experimentally the nature of instabilities and their development into waves and blobs in the simple magnetized toroidal plasmas of the TORPEX device. Linear and non-linear analysis techniques together with statistical and conditional sampling methods are used to gain insight into the physics of plasma turbulence and transport. Further progress in the field will be achieved by applying the same analysis tools to numerical simulations allowing a direct comparison of experiment and theory. Future experiments include the use of a fast framing camera for non-perturbing visible light measurements, which can be correlated and compared with local electrostatic measurements [18]. The interaction between small scale turbulence and fast ions, presently recognized as an open question for burning plasma physics, will also be investigated in TORPEX, taking advantage of the progress accomplished in characterizing the turbulence in different plasma scenarios [19].

This work was supported in part by the *Fonds National Suisse de la Recherche Scientifique*.

References

[1] FASOLI, A., et al., “Electrostatic turbulence and transport in a simple magnetized plasma”, Phys. Plasmas **13** (2006) 055902.

[2] MULLER, S.H., et al., ”Plasma blobs in a basic toroidal experiment: Origin, dynamics, and induced transport”, Phys Plasmas **14** (2007) 110704.

[3] FURNO, I., et al., “Experimental Observation of the Blob-Generation Mechanism from Interchange Waves in a Plasma”, Phys. Rev. Lett. **100** (2008) 055004; FURNO, I., et al., “Mechanism for blob generation in the TORPEX toroidal plasma”, Phys. Plasmas **15** (2008) 055903.

[4] RYPDAL, K., et al.,”Onset of turbulence and profile resilience in the Helimak configuration”, Phys. Rev. Lett. **94** (2005) 225002.

[5] POLI, F.M., et al., “Experimental characterization of drift-interchange instabilities in a simple toroidal plasma”, Phys. Plasmas **13** (2006) 102104; POLI F. M., et al.,”Transition from drift to interchange instabilities in an open magnetic field line configuration”, Phys. Plasmas **15** (2008) 032104**.**

[6] LABIT, B., et al.,”Universal statistical properties of drift-interchange turbulence in TORPEX plasmas”, Phys. Rev. Lett. **98** (2007) 255002; LABIT, B., et al.,”Statistical properties of electrostatic turbulence in toroidal magnetized plasmas”**,** Plasma Phys. Controlled Fusion **49** (2007) B281.

[7] THEILER, C., et al.,”The role of the density gradient on intermittent cross-field transport events in a simple magnetized toroidal plasma”, Phys Plasmas **15** (2008) 042303.

[8] MULLER, S.H., et al., “Probabilistic analysis of turbulent structures from two-dimensional plasma imaging”, Phys. Plasmas **13** (2006) 100701.

[9] KRASHENINNIKOV, S.I., et al., “Recent Theoretical Progress in Understanding Coherent Structures in Edge and SOL Turbulence”, J. Plasma Phys. Published online by Cambridge University Press, 2008, DOI: 10.1017/S0022377807006940.

[10] MYRA, J., et al.,”Blob birth and transport in the tokamak edge plasma: Analysis of imaging data”, Phys. Plasmas **13** (2006) 092509.

[11] DIALLO A., et al., “Dynamics of Plasma Blobs in a Shear Flow”, Phys. Rev. Lett. **101** (2008) 115005.

[12] PODESTÀ, M., et al., “Cross-field transport by instabilities and blobs in a magnetized toroidal plasma”, Phys. Rev. Lett. **101** (2008) 045001.

[13] RICCI, P., et al., “High- and low-confinement modes in simple magnetized toroidal plasmas”**,** Phys. Rev. Lett. **100** (2008) 225002.

[14] ZEILER, A., et al., “Nonlinear reduced Braginskii equations with ion thermal dynamics in toroidal plasma”, Phys. Plasmas **4** (1997) 2134.

[15] STANGEBY, P.C., “The Plasma Boundary of Magnetic Fusion Devices”, (Institute of Physics, Berkshire, 2000).

[16] BISAI, N., “Simulation of plasma transport by coherent structures in scrape-off-layer tokamak plasmas”, Phys. Plasmas **11**, (2004) 4018.

[17] YU, G.Q., “Two-dimensional modeling of blob dynamics in tokamak edge plasmas”, Phys. Plasmas **13** (2006) 042508.

[18] IRAJI, D., et al., “Fast visible imaging of turbulent plasma in TORPEX”, to appear in Rev. Sci Istrum. **79**, Issue 10 (2008).

[19] PLYUSHCHEV, G., et al., “Fast ion source and detector for investigating the interaction of turbulence with suprathermal ions in a low temperature toroidal plasma”, Rev. Sci. Instrum. **77** (2006) 10F503.